Gurung *et al. EPJ Techniques and Instrumentation* (2021) 8:3
https://doi.org/10.1140/epjti/s40485-020-00058-z

EPJ Techniques and Instrumentation

RESEARCH ARTICLE Open Access

Fast decay of 2^3S_1 positronium atoms in an MgO lined cavity

Lokesh Gurung, Tamara J. Babij and David B. Cassidy*

*Correspondence:
d.cassidy@ucl.ac.uk
Department of Physics and Astronomy, University College London, Gower Street, WC1E 6BT London, UK

Abstract

We report experiments in which radiatively metastable $2\,^3S_1$ positronium (Ps) atoms entered a waveguide whose internal surfaces were lined with smoked magnesium oxide (MgO) powder. The waveguide was built such that time-delayed microwave radiation pulses, tuned to drive $2\,^3S_1 \rightarrow 2\,^3P_2$ transitions, could be applied to the Ps ensemble. The lifetime of $2\,^3S_1$ atoms was measured using time-delayed microwave induced decay, yielding $\approx$ 200 ns. This is considerably shorter than the Zeeman shifted lifetime of 1070 ns, indicating that Ps atoms in the $2\,^3S_1$ state do not survive multiple collisions with MgO nanocrystals.

Keywords: Positron, Positronium, Antimatter, QED, Spectroscopy

Introduction

Positronium (Ps) [1] is a hydrogenic atomic system composed of an electron bound to a positron via the Coulomb interaction. As a particle-antiparticle system, Ps is metastable, with a lifetime against annihilation of $\approx$ 142 ns for the 1^3S_1 triplet ground state [2]. The fact that Ps is composed of low mass leptons means that it is, for any experimentally relevant regimes, fully described by quantum electrodynamics (QED). In particular, the absence of any hadronic contribution to its structure means that Ps is the ideal system to test bound-state QED theory [3]. Moreover, since Ps can be fully described by QED, any observed deviation from theory may be an indication of physics not included in the Standard Model [4].

There have been many experimental tests of QED using Ps [5, 6], based primarily on precision measurements of annihilation decay rates [7–10] and energy levels [11–23]. In general experimental results are much less precise than the corresponding theoretical values, and there is therefore a need for more advanced experimentation [24]. Most of the previous precision Ps measurements were performed decades ago, and subsequent technological advances have made it feasible to make significant improvements to these measurements, for example, new positron trapping techniques [25] and laser metrology [26].

One of the fundamental limitations in precision Ps measurements are the Ps atoms themselves: their low mass means that, even at thermal energies, typical speeds are on the order of 10^7 cm/s, and, depending on how the atoms are created, they may well be much faster than this [27]. Unfortunately, progress in producing cold Ps atoms has not advanced in step with other developments, so that, while technological developments have made it possible to improve upon previous measurements, overcoming the limitations caused by using fast and uncontrolled Ps atoms remains a significant challenge.

There are several different experimental problems caused by fast and divergent sources of Ps atoms: Doppler broadening effects can be large, for example single-photon $1\,^3S_1 \rightarrow 2\,^3P_J$ transitions are typically broadened from the 50 MHz natural width to $\approx$ 500 GHz [28]. Even if Doppler-free methods are used to excite Ps atoms, as in two-photon $1\,^3S_1 \rightarrow 2\,^3S_1$ transitions [16], transit time broadening and second order Doppler shifts are still significant. Furthermore, fast Ps atoms will quickly spread out over a large volume, making it more difficult to probe them with lasers, for example in a laser cooling experiment [29]. The work we describe here was undertaken to investigate the possibility of physically confining radiatively metastable $2\,^3S_1$ Ps atoms, in order to mitigate some of these problems. We report the results of experiments in which atoms excited to the $2\,^3S_1$ state were allowed to fly into a WR-112 waveguide whose internal surfaces were lined with magnesium oxide (MgO) nanocrystals. Microwave radiation tuned to drive $2\,^3S_1 \rightarrow 2\,^3P_J$ transitions was used to measure the lifetime of these atoms, yielding on the order of 200 ns. As this is much shorter than the Zeeman shifted lifetime of 1070 ns [2], we conclude that Ps atoms in the $2\,^3S_1$ state do not survive multiple collisions with MgO nanocrystals.

Experimental procedure

Ps production and excitation

The experimental apparatus and measurement techniques used in this work are described in detail elsewhere [30, 31]. A two-stage Surko type buffer gas trap [25], coupled to the moderated output of a ^{22}Na radioactive source, was used to generate a pulsed positron beam containing $\approx 10^5$ positrons, at a rate of 1 Hz, with a temporal and spatial width of 3 ns and 2 mm (FWHM) respectively. The positron beam was transported by an axial magnetic field of strength 100 G and passed through a waveguide before being implanted into a mesoporous silica (SiO_2) target, producing Ps atoms with $\approx$ 30% efficiency [32]. The SiO_2 target was mounted on an aluminium electrode which was electrically insulated from a grid electrode, separated by 7 mm, allowing control of the electric field in the laser excitation region, as indicated in Fig. 1. The grid electrode, through which both positrons and Ps atoms passed, was made from a high transmission tungsten mesh (90%).

Ground state Ps atoms emitted from the silica target were optically excited by radiation generated from a pulsed dye laser, propagating along the x direction. The dye laser, pumped by the third harmonic of a pulsed Nd:YAG laser, generated ultra-violet (UV) light with wavelength $\lambda_{UV} = 243$ nm, pulse energy $E_{pulse} = 0.5$ mJ, and a bandwidth of 100 GHz (FWHM). The 243 nm radiation is resonant with the $1\,^3S_1 \rightarrow 2\,^3P_J$ [28] transitions and covers all three 2^3P_J states due to the large bandwidth of the laser. Metastable $2\,^3S_1$ atoms were generated from the $1\,^3S_1$ ground state using the same single-photon excitation scheme. This transition is forbidden by electric dipole selection rules, but can be driven in an electric field, as discussed in detail elsewhere [33]. Briefly, Ps atoms were generated in

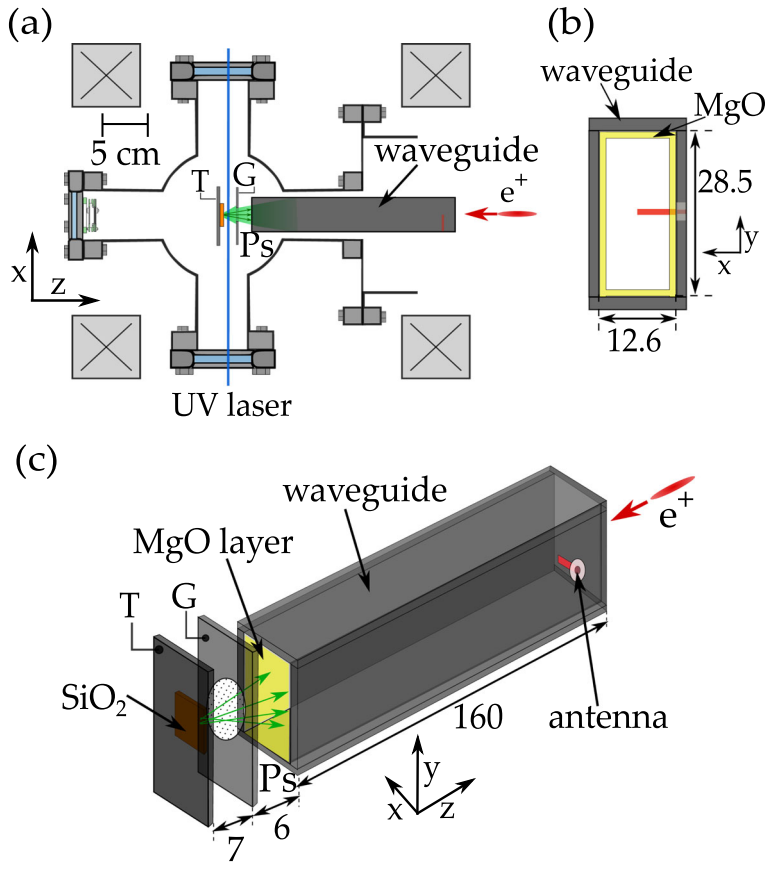

Fig. 1 **a** A schematic of the Ps production region, detectors, and waveguide. **b** A cross-section of the MgO coated WR-112 waveguide in the xy plane. **c** A 3-D schematic of the target, grid, and microwave guide. The target (T) and grid (G) electrodes were mounted on a separate manipulator that could be moved off axis to allow direct imaging of the positron beam after it had passed through the waveguide.The waveguide dimensions are in mm

an initial electric field $F(0)_{\text{ex.}}$ = 5 kV/cm, generated from the bias on target electrode (T = 3.5 keV) and the grid electrode (G = 0V). Immediately after the Ps was produced the target bias was turned off, allowing for a reduced electric field $F(t)_{\text{ex.}} \approx 2$ kV/cm during the subsequent laser excitation. This was accomplished using a fast high-voltage (HV) switch [(90–10% ≈ 30 ns)]. The presence of the electric field results in the creation of a Stark mixed $n = 2$ state, denoted as $2\,^3S'_1$, which possesses both S and P character. The $l = 1$ (2P) character of the mixed state permits the single photon excitation to the $2\,^3S'_1$ state, while the $l = 0$ (2S) character increases the lifetime [31] and allows the system to evolve into pure $2\,^3S_1$ states as the electric field is further reduced [33]. Of all atoms excited to $n = 2$, approximately 5% are expected to end up in pure $2\,^3S_1$ states corresponding to ≈ 1000 atoms per pulse. The 2^3S_1 state is radiatively metastable, with a lifetime against annihilation of 1136 ns. The application of ≈ 100 G field in the excitation region lowers the lifetime to 1070 ns due to Zeeman mixing.

γ-ray spectroscopy

The production and excitation of Ps atoms was monitored using a single-shot lifetime spectroscopy technique [34] that involves the detection of annihilation radiation using

fast detectors. In this work we use lutetium yttrium oxyorthosilicate (LYSO) scintillators coupled to photomultiplier tubes (PMT) via acrylic light guides [31].

The $2\,^3S_1$ Ps states studied in this work are relatively long-lived, and atoms may therefore travel long distances before decaying. This means that the γ-ray detection efficiency could depend on the time, and hence position, at which annihilation occurs. Three detectors (designated D1-3) were used in this work, placed around the target chamber as indicated in Fig. 2. D1 and D2 were placed close to the Ps production region, while D3 was placed further back to mitigate the effect of position-dependent detection efficiency. The detectors D1 and D2 were both made using square LYSO arrays with area 16 cm^2 and thickness 2 cm, whereas the scintillator used in D3 had a circular array with area 45 cm^2 and a thickness of 2 cm.

The γ-ray detectors were connected to an oscilloscope that recorded the time dependent PMT anode voltage $V(t)$ following implantation of a positron pulse into a target. The measured signal constitutes a lifetime spectrum, convoluted with the system response [34]. For LYSO based detectors this response is dominated by the $\approx$ 40 ns scintillator decay time. Figure 3a shows examples of such lifetime spectra, recorded with the positron beam implanted into a silica target. Spectra of this type are typically obtained by averaging several hundred individual shots.

Any processes that change the decay rate of Ps atoms can be observed in the difference between lifetime spectra with and without the perturbing effect present. Examples of such difference spectra are shown in Fig. 3b for two different cases. Photoionization results

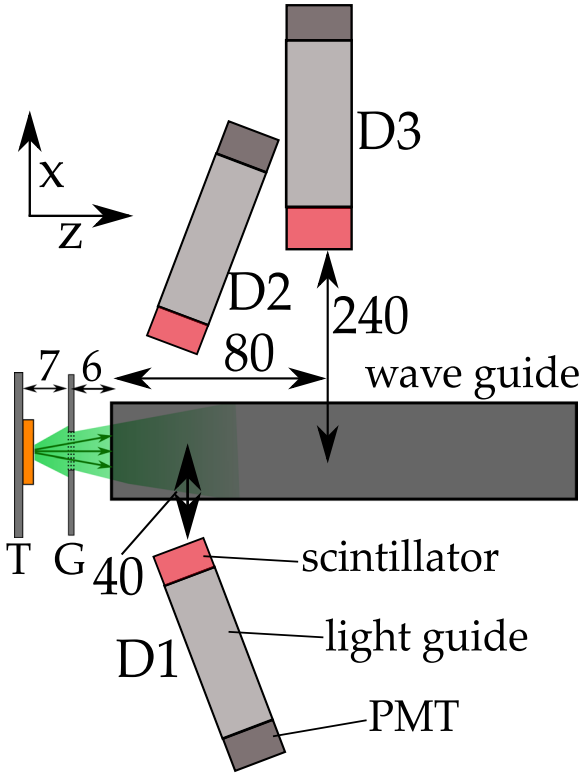

Fig. 2 Schematic positions of the three γ-ray detectors relative to the waveguide structure (not to scale). D1 and D2 were symmetrically placed near the Ps production region, and D3 was located further away, with a field of view covering the entire waveguide region. All dimensions are in mm

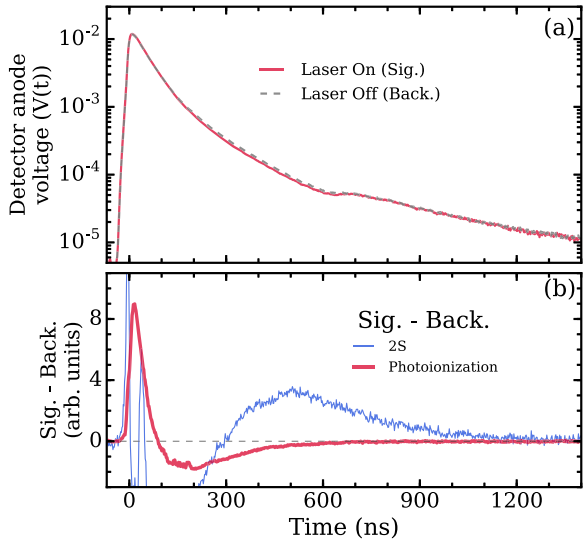

Fig. 3 **a** Example of lifetime spectra taken with LYSO detector for 3.5 keV positrons impinging on SiO_2 (Sig. and Back.) and, **b** Background subtracted spectra showing examples of photoionization, and $2\,^3S_1$ production, as described in the text. The signal and background spectra in (**a**) correspond to the photoionization signal in (**b**)

in earlier annihilation events relative to the ground state lifetime (142 ns), and thus an early peak in the background subtracted spectrum is observed (where the background spectrum is recorded with no laser light present). Conversely, excitation of Ps to long-lived $2\,^3S_1$ states results in a later peak in the difference spectrum. These positive peaks are accompanied by negative troughs elsewhere in the difference spectra, corresponding to a reduction in the number of annihilation events with respect to the ground state Ps decay. The negative or positive aspects of the difference spectra may appear earlier or later in the spectrum, depending on whether Ps decay events are made to happen earlier (as in photoionization) or later (as in $2\,^3S_1$ production).

The amount of Ps present can be quantified by integrating lifetime spectra over appropriate time windows [34], but in this work we use time-delayed microwave induced decays [35]. This technique works by driving resonant $2\,^3S_1 \rightarrow 2\,^3P_2$ transitions with pulsed microwave radiation. The resulting $2\,^3P_2$ states decay radiatively to the $1\,^3S_1$ ground state with a lifetime of 3.2 ns, and the amplitude of the subsequent annihilation radiation peak is used as a measure of the number of $2\,^3S_1$ atoms remaining at the time of the radiation pulse. Thus, by changing the times at which microwave pulses were applied, lifetime spectra may be generated. An example of data obtained in this way is shown in Fig. 4. A smoothing function was applied to the curves in order to determine the peak amplitude at a fixed time (70 ns) after the application of the microwave pulse.

Microwave guide and MgO preparation

The quenching of the metastable atoms via the $2\,^3S_1 \rightarrow 2\,^3P_2$ transition, resonant at 8.626 GHz, was performed in a WR-112 microwave guide with dimensions of 12.6 $\times$28.5 $\times$ 160 mm as illustrated in Fig. 1. The radiation input at the waveguide antenna was set to be ν = 8.626 GHz and P_{Input} = 320 mW, with the trigger times controlled by an external generator. The inner surface of the waveguide was coated with MgO powder [36]. To coat the waveguide, $\approx$ 0.8 g strips of Mg ribbon were combusted in air, and the resulting smoke

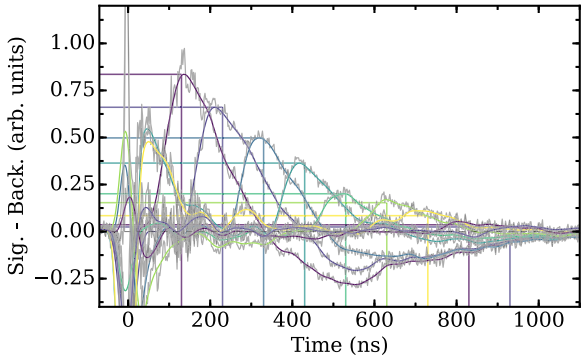

Fig. 4 Difference spectra showing the microwave induced annihilation peaks. The solid curves are obtained after applying a Savitzky-Golay smoothing function to the data. The horizontal lines represent the peak amplitude values obtained from the smoothed data and the vertical lines indicate the corresponding quench times

was deposited on the disassembled waveguide surfaces as shown in Fig. 5a, held ∼15 cm from the source. The waveguide was then carefully assembled as shown in Fig. 5b and installed in the vacuum system, avoiding disruption of the MgO layer. Simulations using the CST software package indicate that the MgO layer will have no significant effect on the microwave radiation field in the waveguide.

Smoked MgO powder produced by Mg combustion in air is known to be composed of cubic MgO nanocrystals, with edge lengths varying from 10 nm to 1 μm [37]. Figure 6 shows a scanning electron micrograph of a similarly prepared MgO layer (on a Cu substrate). Previous measurements of Ps produced in MgO layers made in the same way indicate that the layer thickness is on the order of 30 μm [36]. Before implantation into the silica target, the positron beam passed through the waveguide via a 7 mm aperture. As MgO is an insulator, it is possible that the internal waveguide surfaces could become electrically charged and deflect the positron beam. After passing through the waveguide the positron beam was imaged on a multi-channel plate (MCP) detector (see Fig. 1a), and no beam deflection was observed over the course of the measurements.

Results and discussion

Lifetime spectra were produced from microwave quenching data similar to those shown in Fig. 4. For each spectrum the amplitudes of the smoothed peaks were evaluated at

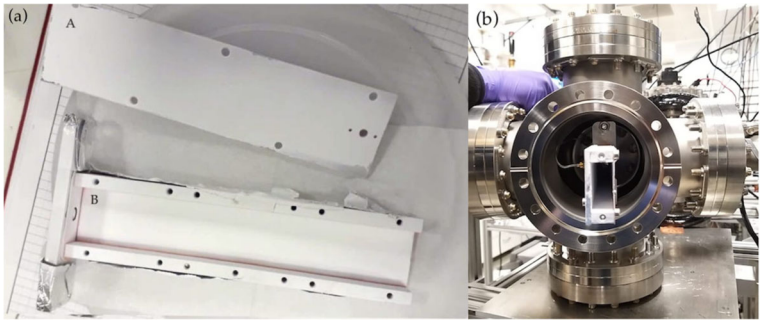

Fig. 5 **a** The MgO smoke powder lined waveguide parts prior to assembly. Part A is screwed onto part B. **b** The assembled waveguide mounted inside the target chamber

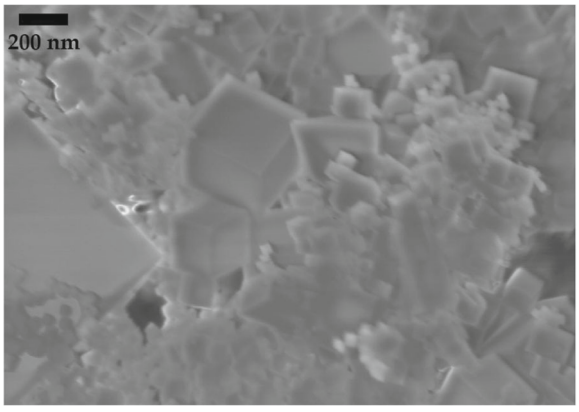

Fig. 6 A scanning electron microscopy (SEM) image of MgO smoke nanocrystals taken by a Karl Zeiss XB1540 microscope with a 3 keV electron beam. The large variation in the edge lengths of the cubic crystals, (10-1000 nm [37]) is visible

100 ns intervals corresponding to the times at which the microwave radiation pulses were applied, taking into account a 70 ns delay between the application of the microwave pulse and the peak amplitude of the subsequent annihilation pulse. This delay is due to the ground state decay rate and the LYSO detector response. The amplitude data plotted for each time step are shown in Fig. 7 for each of the three detectors D1-3, along with a simple with an exponential fit, which yielded lifetimes on the order of 200 ns. It should

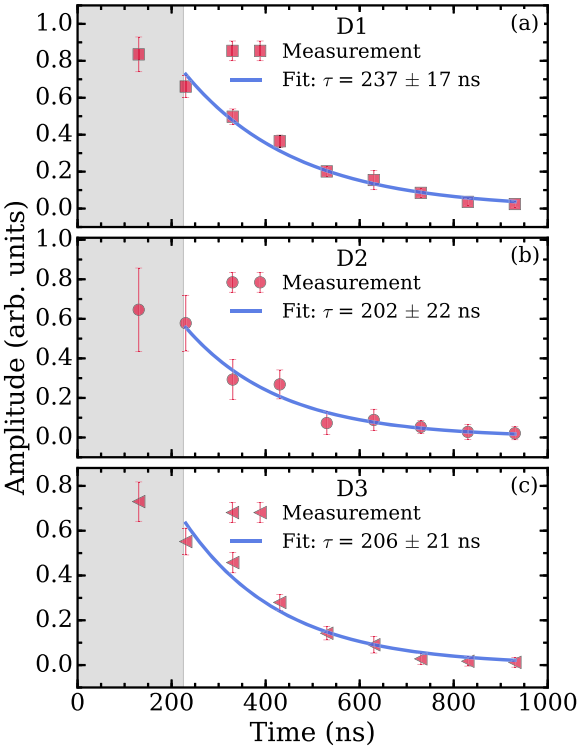

Fig. 7 Lifetime spectra for $2\,^3S_1$ atoms obtained from smoothed quenching data using detectors D1-3, as explained in the text. The solid curves are exponential fits to the data. The grey bands represent the region in which data are not used in the fit since it takes 200 ns until all atoms have entered the waveguide

be pointed out that there is no reason to expect the collision (and hence decay) rate to be exponential, and thus the quoted lifetimes, which are derived from exponential fits, should be considered estimates at best. Nevertheless, it is clear that the $2\,^3S_1$ lifetimes are considerably shorter than the expected 1070 ns.

In principle the Ps atoms could travel the entire length of the waveguide before being quenched. Ps atoms emitted from SiO_2 targets are expected to mean longitudinal speeds of order 10^7 cm/s [38], meaning that it would take around 1.6 μs to leave the guide (not taking into account the effects of scattering from random nanocrystal surface orientations, which can only increase the transit times). As atoms travel further from the source, the detection efficiency for detectors D1 and D2 would decrease, owing to the decreasing solid angle subtended; this would make the apparent lifetime shorter. However, D3 was located in a position that would be less sensitive to this effect. Moreover, the D3 geometrical detection efficiency would initially increase until atoms reached half way along the waveguide. Although the lifetimes obtained from the data shown in Fig. 7 are not expected to be very accurate, the fact that they are all essentially the same indicates that Ps atoms do not annihilate over a large volume, so that while D1 and D2 may have a different effective solid angle coverage to that of D3, there does not appear to be a strong time dependence, which is consistent with a short Ps lifetime.

Ps atoms in pure $2\,^3S_1$ states entered the microwave guide as shown in Fig. 1. The laser excitation process means that Ps atoms have a relatively narrow velocity spread in the x direction as a result of the 100 GHz laser bandwidth. However the velocity distribution in the y direction is much broader (FWHM $\approx$ 500 GHz) [39], meaning that a large fraction of Ps atoms can be expected to collide with the internal waveguide surfaces. After such collisions the Ps atoms may reflect from the nano crystals with randomized trajectories, in accordance with the random cube orientations (see Fig. 6). This means that Ps atoms may be reflected back into the wavegude immediately, or after multiple scattering events in the inner structure of the MgO layer.

The short observed lifetime of $2\,^3S_1$ atoms indicates that Ps atoms do not survive collisions with MgO nanocrystals. Excited state Ps atoms created in MgO samples have been studied in previous experiments [40]. In that work Ps atoms were generated and excited inside MgO powder samples and were then able to travel into vacuum after scattering from the internal MgO crystal surfaces. However, $2\,^3S_1$ states were not measured as the single-photon production method used here [33] is not compatible with the formation of atoms in the MgO powder. Atoms excited to $2\,^3P_J$ states and to Rydberg states with principal quantum numbers n ranging from 10–17 were studied; It was found that the $1\,^3S_1$ ground state and the $2\,^3P_J$ energy levels were shifted, but that Rydberg levels were not [40]. Since Rydberg atoms are extremely sensitive to electric fields [41] we can conclude from this that MgO does not support electric fields strong enough to quench $2\,^3S_1$ atoms. Even if the field were localized to the surface region, Rydberg atoms excited with low positron beam implantation energy would sample the near surface region, and would therefore be sensitive to these fields. No such level shifts were observed for Rydberg states, however, and it does not appear that the short lifetime observed in this work was caused by electric fields.

It is possible that interactions with surfaces lead to decay via pick-off annnihilation, which is the process wherein the positron in a Ps atom annihilates with an external electron in the surrounding medium rather than by self-annihilation [42]. Gidley and

co-workers have previously used MgO lined cavities to contain ground state Ps atoms for precision decay rate measurements [43]. The rationale for this approach was that Ps-MgO interactions would lead to only a small increase in the annihilation rate, based on earlier measurements of long-lived Ps in several insulating materials [44]. It was found, however, that high-precision measurements were still sensitive to Ps-MgO interactions, which therefore had to be taken into account before agreement with QED theory was obtained [8, 9]. Nevertheless, the effect of MgO interactions was shown to be relatively small, and was only noticed because of the high precision of the measurements (of order ppm).

If the pick-off process is responsible for the present observed lifetimes, it would imply that $2\,^3S_1$ atoms are orders of magnitude more sensitive to interactions with MgO surfaces than $1\,^3S_1$ atoms. However, it is not clear why Rydberg atoms would not also be susceptible to the same decay mechanisms, and in fact one would expect them to be even more sensitive than $2\,^3S_1$ atoms, given that the electron and positron are less strongly bound. However, Rydberg atoms generated in MgO powder were able to leave without significant losses [40], and it therefore does not seem likely that an enhanced pick-off rate is responsible for the present observations.

It is known from Ps beam experiments [45] that when Ps atoms scatter from atoms and molecules they become polarized during the collision [46, 47]. This means that the pure $2\,^3S_1$ states may acquire some P character, facilitating faster (radiative) decay [31]. However, for a direct scattering process one would expect the interaction time to be much less than the 3.2 ns $2\,^3P_J$ lifetime, and so for adiabatic interactions this mechanism would not significantly change the decay rate unless the scattering rates were correspondingly high. The MgO structure (see Fig. 6) contains large open volumes, which is why the ground state Ps lifetime in bulk MgO samples is close to the vacuum lifetime [44]. In previous measurements ground state Ps atoms were observed to travel through $\approx 30\ \mu$m thick layers of MgO [36] without measurable time delays or losses compared to passing through a few hundred nm of the same sample. These data suggest that the large open areas in MgO samples allow Ps atoms to pass through with only a small number of collisions. Thus, we would not expect a small increase in the decay rate due to impulse polarization to be enhanced by a large number of collisions, and thence lead to the short observed $2\,^3S_1$ lifetimes.

The previously observed energy shifts indicated that resonant interactions between Ps atoms and MgO surfaces can be mediated via photo-luminescent MgO absorption bands [40]. The associated energy shifts were observed for atoms that were mostly not in a near surface region, which was taken to be evidence for a strong coupling with multiple MgO absorbers, giving rise to a much stronger interaction. It is therefore possible that when $2\,^3S_1$ atoms scatter from MgO nanocrystal surfaces they become polarized, and are then able to interact via this same mechanism. The increased strength of this interaction compared to a simple scattering process could then lead to a non-adiabatic process that transfers population to the $2\,^3P_J$ levels, with a concomitant reduction in the observed lifetime. Further studies are required to determine if this is in fact the mechanism responsible for our observations, including testing other insulating surface materials.

An insulating cavity has been used to physically confine excited state atoms in recent measurements of $1\,^3S_1 \rightarrow 2\,^3S_1$ transitions [48]. In this case a relatively small (≈ 3 mm path length) silica lined cavity was used to confine Ps atoms, and allow them to make multiple passes through a narrow laser beam (0.37 mm waist) so as to increase the total

interaction time. The production of $2\,^3S_1$ atoms was observed using a lifetime method sensitive to decay events in a time window of 2-4 μs after the positron implantation, which implies that the $2\,^3S_1$ lifetime was not as short as in the present measurement, although it was not possible to determine the actual lifetime from the data presented in [48]. Nevertheless, these data could mean that interactions of $2\,^3S_1$ Ps atoms with MgO and silica are different. This could be the case if the energy shifting interaction observed for MgO [40] is not present in amorphous silica. We note also that spatial confinement of muonium atoms using silica cavities has been demonstrated [49].

Conclusions

The attempt to make a confining structure for $2\,^3S_1$ Ps atoms was not successful, and we found instead that these atoms do not survive interactions with surfaces lined with MgO smoke powder. Previous experiments [40, 43] have indicated that both $1\,^3S_1$ ground state atoms and Rydberg atoms (with n = 10-18) do survive such interactions, and we suggest that $2\,^3S_1$ atoms behave differently because they can be quenched by ℓ-mixing. However, measurements with Rydberg atoms, which are highly sensitive to electric fields, indicates that the MgO does not charge up, and that there are no large electric fields present [40]. Instead, the mixing may be mediated by coupling to multiple MgO absorbers via a previously observed mechanism [40], providing a more efficient route to quenching. This makes MgO powder an unsuitable material for physical confinement of $2\,^3S_1$ atoms, although this does not necessarily mean that other materials cannot be used to achieve this goal as they may not support the same quenching mechanisms.

Abbreviations

Ps: Positronium; MgO: Magnesium Oxide; QED: Quantum Electrodynamics; UV: Ultra-violet; HV: High-voltage; LYSO: Lutetium Yttrium Oxyorthosilicate; PMT: Photomultiplier Tubes; MCP: Multi-Channel Plate

Acknowledgements

We gratefully acknowledge L. Liszkay for providing silica samples, S. Huo from the London Centre for Nanotechnology for assistance with the SEM imaging, S. D. Hogan and P. Crivelli for helpful discussions, and R. E. Sheldon, J. Dumper and R. Jawad for technical assistance.

Authors' contributions

LG and DBC drafted the manuscript. LG, TJB, and DBC conceived and constructed the experiment. LG acquired and analyzed the data. TJB performed the CST simulations. All authors contributed to the interpretation of the results. The manuscript was read and approved by all authors.

Funding

This work was supported by the EPSRC under Grant No. EP/R006474/1.

Availability of data and materials

The datasets used and/or analyzed during the current study are available from the corresponding author on reasonable request.

Competing interests

The authors declare there are no competing interests.

Received: 19 September 2020 Accepted: 15 December 2020
Published online: 15 January 2021

References

1. Wheeler JA. Polyelectrons. Annals of the New York Academy of Sciences. 1946;48(3):219–38. https://doi.org/10.1111/j.1749-6632.1946.tb31764.x.
2. Ore A, Powell JL. Three-Photon Annihilation of an Electron-Positron Pair. Phys Rev. 1949;75:1696–9. https://doi.org/10.1103/PhysRev.75.1696.
3. Karshenboim SG. Precision study of positronium: testing bound state QED theory. Int J Mod Phys A. 2004;19(23):3879–96. https://doi.org/10.1142/S0217751X04020142.
4. Safronova MS, Budker D, DeMille D, Kimball DFJ, Derevianko A, Clark CW. Search for new physics with atoms and molecules. Rev Mod Phys. 2018;90:025008. https://doi.org/10.1103/RevModPhys.90.025008.

5. Berko S, Pendleton HN. Positronium. Annu Rev Nucl Part Sci. 1980;30(1):543–81. https://doi.org/10.1146/annurev.ns.30.120180.002551.
6. Rich A. Recent experimental advances in positronium research. Rev Mod Phys. 1981;53(1):127. https://doi.org/10.1103/RevModPhys.53.127.
7. Al-Ramadhan AH, Gidley DW. New precision measurement of the decay rate of singlet positronium. Phys Rev Lett. 1994;72:1632–5. https://doi.org/10.1103/PhysRevLett.72.1632.
8. Vallery RS, Zitzewitz PW, Gidley DW. Resolution of the Orthopositronium-Lifetime Puzzle. Phys Rev Lett. 2003;90:203402. https://doi.org/10.1103/PhysRevLett.90.203402.
9. Jinnouchi O, Asai S, Kobayashi T. Precision measurement of orthopositronium decay rate using SiO_2 powder. Phys Lett B. 2003;572:117–26. https://doi.org/10.1016/j.physletb.2003.08.018.
10. Kataoka Y, Asai S, Kobayashi T. First test of order α^2 correction of the orthopositronium decay rate. Physics Letters B. 2009;671(2):219–23. https://doi.org/10.1016/j.physletb.2008.12.008.
11. Deutsch M, Brown SC. Zeeman Effect and Hyperfine Splitting of Positronium. Phys Rev. 1952;85:1047–8. https://doi.org/10.1103/PhysRev.85.1047.
12. Mills Jr. AP, Bearman GH. New measurement of the positronium hyperfine interval. Phys Rev Lett. 1975;34:246–50. https://doi.org/10.1103/PhysRevLett.34.246.
13. Ritter MW, Egan PO, Hughes VW, Woodle KA. Precision determination of the hyperfine-structure interval in the ground state of positronium. V. Phys Rev A. 1984;30:1331–8. https://doi.org/10.1103/PhysRevA.30.1331.
14. Ishida A, Namba T, Asai S, Kobayashi T, Saito H, Yoshida M, Tanaka K, Yamamoto A. New precision measurement of hyperfine splitting of positronium. Phys Lett B. 2014;734:338–44.
15. Chu S, Mills Jr. AP. Excitation of the Positronium $1\,^3S_1 \rightarrow 2\,^3S_1$ Two-Photon Transition. Phys Rev Lett. 1982;48:1333–7. https://doi.org/10.1103/PhysRevLett.48.1333.
16. Chu S, Mills Jr. AP, Hall JL. Measurement of the positronium $1\,^3S_1 \rightarrow 2\,^3S_1$ interval by doppler-free two-photon spectroscopy. Phys Rev Lett. 1984;52:1689–92. https://doi.org/10.1103/PhysRevLett.52.1689.
17. Fee MS, Mills Jr. AP, Chu S, Shaw ED, Danzmann K, Chichester RJ, Zuckerman DM. Measurement of the positronium $1\,^3S_1 \rightarrow 2\,^3S_1$ interval by continuous-wave two-photon excitation. Phys Rev Lett. 1993;70:1397–1400. https://doi.org/10.1103/PhysRevLett.70.1397.
18. Fee MS, Chu S, Mills Jr. AP, Chichester RJ, Zuckerman DM, Shaw ED, Danzmann K. Measurement of the positronium $1\,^3S_1 \rightarrow 2\,^3S_1$ interval by continuous-wave two-photon excitation. Phys Rev A. 1993;48:192–219. https://doi.org/10.1103/PhysRevA.48.192.
19. Mills Jr. AP, Berko S, Canter KF. Fine-Structure Measurement in the First Excited State of Positronium. Phys Rev Lett. 1975;34:1541–4. https://doi.org/10.1103/PhysRevLett.34.1541.
20. Hatamian S, Conti RS, Rich A. Measurements of the $2^3S_1 - 2^3P_J (J = 0, 1, 2)$ fine-structure splittings in positronium. Phys Rev Lett. 1987;58:1833–6. https://doi.org/10.1103/PhysRevLett.58.1833.
21. Hagena D, Ley R, Weil D, Werth G, Arnold W, Schneider H. Precise measurement of n =2 positronium fine-structure intervals. Phys Rev Lett. 1993;71:2887–90. https://doi.org/10.1103/PhysRevLett.71.2887.
22. Conti RS, Hatamian S, Lapidus L, Rich A, Skalsey M. Search for C-violating, P-conserving interactions and observation of 2^3S_1 to 2^1P_1 transitions in positronium. Phys Lett A. 1993;177(1):43–8. https://doi.org/10.1016/0375-9601(93)90371-6.
23. Cassidy DB, Hisakado TH, Tom HWK, Mills Jr. AP. Positronium hyperfine interval measured via saturated absorption spectroscopy. Phys Rev Lett. 2012;109:073401. https://doi.org/10.1103/PhysRevLett.109.073401.
24. Ley R. Atomic physics of positronium with intense slow positron beams. Appl Surf Sci. 2002;194:301–6. https://doi.org/10.1016/S0169-4332(02)00139-3.
25. Danielson JR, Dubin DHE, Greaves RG, Surko CM. Plasma and trap-based techniques for science with positrons. Rev Mod Phys. 2015;87:247–306. https://doi.org/10.1103/RevModPhys.87.247.
26. Udem T, Holzwarth R, Hansch TW. Optical frequency metrology. Nature. 2002;416(6877):233–7.
27. Cassidy DB. Experimental progress in positronium laser physics. Eur Phys J D. 2018;72(3):53. https://doi.org/10.1140/epjd/e2018-80721-y.
28. Cassidy DB, Crivelli P, Hisakado TH, Liszkay L, Meligne VE, Perez P, Tom HWK, Mills Jr. A. P. Positronium cooling in porous silica measured via Doppler spectroscopy. Phys Rev A. 2010;81:012715. https://doi.org/10.1103/PhysRevA.81.012715.
29. Liang EP, Dermer CD. Laser cooling of positronium. Opt Commun. 1988;65(6):419–24. https://doi.org/10.1016/0030-4018(88)90116-2.
30. Cooper BS, Alonso AM, Deller A, Wall TE, Cassidy DB. A trap-based pulsed positron beam optimised for positronium laser spectroscopy. Rev Sci Instrum. 2015;86(10):. https://doi.org/10.1063/1.4931690.
31. Alonso AM, Cooper BS, Deller A, Hogan SD, Cassidy DB. Positronium decay from $n = 2$ states in electric and magnetic fields. Phys Rev A. 2016;93:012506. https://doi.org/10.1103/PhysRevA.93.012506.
32. Liszkay L, Corbel C, Perez P, Desgardin P, Barthe M-F, Ohdaira T, Suzuki R, Crivelli P, Gendotti U, Rubbia A, Etienne M, Walcarius A. Positronium reemission yield from mesostructured silica films. Appl Phys Lett. 2008;92(6):063114. https://doi.org/10.1063/1.2844888.
33. Alonso AM, Hogan SD, Cassidy DB. Production of 2^3S_1 positronium atoms by single-photon excitation in an electric field. Phys Rev A. 2017;95:033408. https://doi.org/10.1103/PhysRevA.95.033408.
34. Cassidy DB, Deng SHM, Tanaka HKM, Mills Jr. AP. Single shot positron annihilation lifetime spectroscopy. Appl Phys Lett. 2006;88(19):194105. https://doi.org/10.1063/1.2203336.
35. Cooper BS, Boilot J-P, Corbel C, Guillemot F, Gurung L, Liszkay L, Cassidy DB. Annihilation of positronium atoms confined in mesoporous and macroporous SiO_2 films. Phys Rev B. 2018;97:205302. https://doi.org/10.1103/PhysRevB.97.205302.
36. Gurung L, Alonso AM, Babij TJ, Cooper BS, Shluger AL, Cassidy DB. Positronium emission from MgO smoke nanocrystals. J Phys B At Mol Opt Phys. 2019;52(10):105004. https://doi.org/10.1088/1361-6455/ab0f06.
37. Jokes CF, Segall RL, Smart RSC, Turner PS. Size distribution of MgO smoke particles. Phil Mag A. 1980;42(2):267–70. https://doi.org/10.1080/01418618009365816.

38. Rayment MH, Gurung L, Sheldon RE, Hogan SD, Cassidy DB. Multiring electrostatic guide for Rydberg positronium. Phys Rev A. 2019;100:013410. https://doi.org/10.1103/PhysRevA.100.013410.
39. Deller A, Cooper BS, Wall TE, Cassidy DB. Positronium emission from mesoporous silica studied by laser-enhanced time-of-flight spectroscopy. New J Phys. 2015;17(4):043059.
40. Gurung L, Cooper BS, Hogan SD, Cassidy DB. Resonant shifts of positronium energy levels in MgO powder. Phys Rev A. 2020;101:012701. https://doi.org/10.1103/PhysRevA.101.012701.
41. Gallagher TF. Rydberg Atoms. Cambridge: Cambridge University Press; 1994.
42. Charlton M, Humberston JW. Positron Physics, 1st edn. Cambridge Monographs on Atomic, Molecular and Chemical Physics - Volume II. Cambridge: Cambridge University Press; 2001.
43. Gidley DW, Zitzewitz PW. Measurement of the vacuum decay rate of orthopositronium formed in an MgO-lined cavity. Phys Lett A. 1978;69(2):97–9. https://doi.org/10.1016/0375-9601(78)90368-7.
44. Paulin R, Ambrosino G. Annihilation libre de l'ortho-positonium formé dans certaines poudres de grande surface spécifique. J Phys France. 1968;29(4):263–70. https://doi.org/10.1051/jphys:01968002904026300.
45. Laricchia G, Armitage S, Kövér Á, Murtagh DJ. Ionizing collisions by positrons and positronium impact on the inert atoms. In: Advances in Atomic, Molecular, and Optical Physics, vol. 56. Academic Press; 2008. p. 1–47. https://doi.org/10.1016/S1049-250X(08)00010-4.
46. Fabrikant II, Gribakin GF. Similarity between positronium-atom and electron-atom scattering. Phys Rev Lett. 2014;112:243201. https://doi.org/10.1103/PhysRevLett.112.243201.
47. Shipman M, Brawley SJ, Sarkadi L, Laricchia G. Resonant scattering of positronium as a quasifree electron. Phys Rev A. 2017;95:032704. https://doi.org/10.1103/PhysRevA.95.032704.
48. Cooke DA, Crivelli P, Alnis J, Antognini A, Brown B, Friedreich S, Gabard A, Haensch TW, Kirch K, Rubbia A, Vrankovic V. Observation of positronium annihilation in the $2S$ state: towards a new measurement of the $1S$-$2S$ transition frequency. Hyperfine Interactions. 20151–7. https://doi.org/10.1007/s10751-015-1158-4.
49. Khaw KS, Antognini A, Prokscha T, Kirch K, Liszkay L, Salman Z, Crivelli P. Spatial confinement of muonium atoms. Phys Rev A. 2016;94:022716. https://doi.org/10.1103/PhysRevA.94.022716.

Publisher's Note